

Controlled source electromagnetic interferometry by multidimensional deconvolution: Spatial sampling aspects

Jürg Hunziker, Evert Slob & Kees Wapenaar

TU Delft, The Netherlands

ABSTRACT

We review electromagnetic interferometry by multidimensional deconvolution (MDD) and investigate its sensitivity to spatial sampling. Two Sea Bed Logging datasets were modeled numerically. One represents a shallow sea situation with a small vertical source-receiver distance and the other a deep sea situation with a large vertical source-receiver distance. The reflection response from below the receivers was retrieved by interferometry by MDD after decomposition of the field into up- and downgoing fields. This reflection response is independent of any effects of the water layer and the air above and consequently the same for the shallow sea and the deep sea situation. We showed, that to decompose the fields and apply MDD successfully for a shallow sea situation a denser sampling is necessary than for a deep sea situation.

Key words: Controlled Source Electromagnetics (CSEM), Sea Bed Logging (SBL), Interferometry, Multidimensional Deconvolution (MDD)

1 INTRODUCTION

In seismics, interferometry is known as the process of cross-correlating two traces at two receiver positions to retrieve the Green's function between these two receivers. The theory has been derived by various authors for a lossless medium (Wapenaar (2004), Schuster *et al.* (2004)) and for a dissipative medium (Snieder, 2006) and it has been applied in passive (Draganov *et al.*, 2006) as well as in active seismics (Bakulin & Calvert, 2006). A more complete overview on seismic interferometry can be found in Wapenaar *et al.* (2008c) or Schuster (2009). Interferometry by crosscorrelation has also been derived for electromagnetics (Slob *et al.*, 2007).

It has been shown that the process of cross-correlation can be replaced by a multi-dimensional deconvolution (MDD) in the controlled-source case (Wapenaar *et al.*, 2008b) and in the passive case (Wapenaar *et al.*, 2008a). The advantages of MDD include elimination of the source signature, improved radiation characteristics of the retrieved source and relaxation of the assumption of a lossless medium. On the other hand, MDD is more expensive and the matrix inversion in-

olved may be unstable. Furthermore a decomposition of the measured fields into up- and downgoing fields is necessary. Interferometry by MDD also requires an array or a network of sensors and can not be done with two receivers only, as this is the case in interferometry by cross-correlation.

In this paper Controlled Source Electromagnetic (CSEM) data in a marine environment is considered. This is often referred to as Sea Bed Logging (SBL), where an electric-dipole source is towed behind a boat emitting a low-frequency electric field, which propagates through the subsurface and through the water. The resulting EM-field is recorded at the ocean bottom by horizontal multicomponent receivers as a function of offset. At small source-receiver offsets the field is dominated by the direct field and reflections from the sea surface. At large offsets the refraction from the sea surface (air-wave) is very strong (Amundsen *et al.*, 2006). Consequently the recorded signal depends on the thickness of the water layer.

By applying interferometry by MDD the source is redatumed to the receiver level, the direct field is eliminated and the water layer is replaced by a vertically

homogeneous overburden (Wapenaar *et al.*, 2008b). In other words, all effects of the water layer, including the dependence on its thickness, are removed. In this paper the necessary receiver spacing for a successful decomposition and subsequent MDD is investigated for a deep and a shallow sea configuration and for a point source using numerical examples.

2 THEORY

The multicomponent electromagnetic fields are decomposed into up- and downgoing fields $\hat{P}^-(x_R, x_S)$ and $\hat{P}^+(x_R, x_S)$, respectively, using an algorithm derived by Slob (2009). The receiver coordinates are represented by x_R and the source coordinates by x_S . The decomposition can be done at any depth level where no sources are present. The implementation used here assumes the material parameters to be laterally constant at the depth level of decomposition. The decomposed fields are related to each other through the reflection response $\hat{R}_0^+(x_R, x'_R)$:

$$\hat{P}^-(x_R, x_S) = \int_{\partial D_R} \hat{R}_0^+(x_R, x'_R) \hat{P}^+(x'_R, x_S) dx'_R, \quad (1)$$

where the integration is taken over all receivers and the circumflex denotes space-frequency domain. The superscript $+$ in the reflection response indicates that its origin is a downgoing field and the subscript 0 represents the absence of heterogeneities above the receiver level. This equation can be rewritten in matrix notation (Berkhout, 1982) as

$$\hat{\mathbf{P}}^- = \hat{\mathbf{R}}_0^+ \hat{\mathbf{P}}^+. \quad (2)$$

Interferometry by MDD solves equation 2 for $\hat{\mathbf{R}}_0^+$ in a least-squares sense:

$$\hat{\mathbf{R}}_0^+ = \hat{\mathbf{P}}^- \left(\hat{\mathbf{P}}^+ \right)^\dagger \left[\hat{\mathbf{P}}^+ \left(\hat{\mathbf{P}}^+ \right)^\dagger + \varepsilon^2 \mathbf{I} \right]^{-1}. \quad (3)$$

The superscript \dagger denotes complex-conjugation and transposition and \mathbf{I} is the identity matrix. The stabilization parameter ε prevents instabilities in the inversion. The retrieved $\hat{\mathbf{R}}_0^+$ is the field with a source at the receiver level, without a direct field and with the water layer replaced with a halfspace consisting of the same material as the first layer below the water.

3 MODELING AND PROCESSING

Two 2D Transverse Magnetic SBL-datasets are modeled in the wavenumber-domain. Consequently there is a J_x source generating a monochromatic signal at a frequency of 0.5 Hz and E_x and H_y receivers recording the resulting earth response. Here J stands for an electric source whose antenna orientation is given by the subscript. The electric and magnetic field components

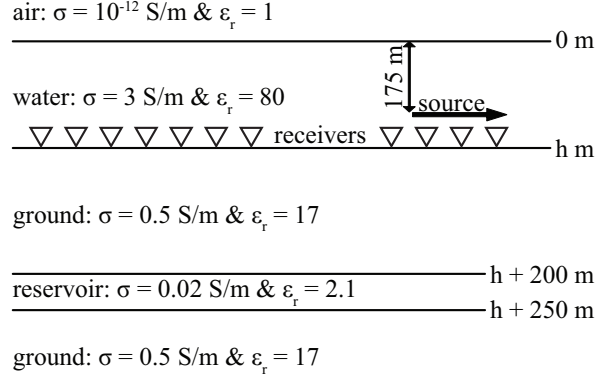


Figure 1. Setup of numerical modeling: The black arrow indicates the source, white triangles the receivers. Conductivity σ and relative permittivity ε_r are given in the according layer.

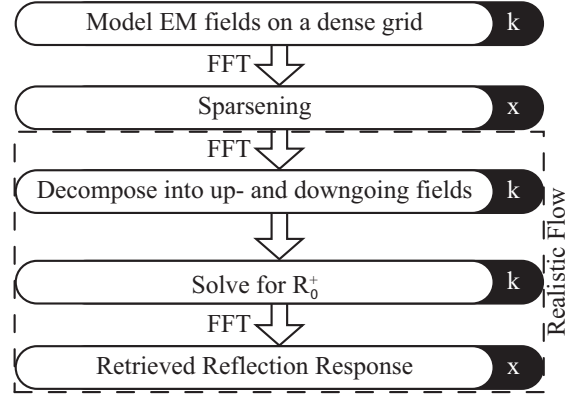


Figure 2. Processing flow: The dashed box labeled Realistic Flow contains all the steps that would be applied to a real dataset. The letters x and k on black ground indicate space and wavenumber-domain, respectively.

are represented by E and H , respectively. Their receiver component is indicated by the subscript. The source is modeled as a point source. The datasets are obtained in a configuration that consists from top to bottom of a halfspace of air, a water layer and halfspace of ground. The latter is intersected by a reservoir layer. The difference between the two datasets is the thickness of the water layer h , which is 200 m in one case to simulate a shallow sea environment and 1000 m in the other case, standing for a deep sea situation. The source is located 175 m below the sea surface. Consequently the vertical source-receiver distance z_{sr} is 25 m for the shallow sea situation and 825 m for the deep sea situation. All the electrical and geometrical parameters are given in figure 1.

After modeling, the datasets are inverse-Fourier transformed to the space-domain, where samples are deleted to create more sparse datasets. Then the

datasets are decomposed into up- and downgoing fields in the wavenumber-domain. Since the medium is laterally invariant, equation 3 can be solved efficient in the wavenumber-domain, where MDD becomes a simple division. The inverse-Fourier transformed result is equivalent with $\hat{\mathbf{R}}_0^+$ retrieved by MDD. The complete processing flow is shown in figure 2.

4 RESULTS

The magnitude of the two electromagnetic field components H_y and E_x are shown in figure 3 in a semi logarithmic plot. The shallow sea situation is plotted with a gray line and the deep sea situation with a lighter gray line. The slope of the curve representing the shallow sea case is steeper at small offsets for both field components than in the deep sea case, because in the deep sea situation the source is vertically further away from the receivers than in the shallow sea situation. Note that the horizontal tails of the electric field between approximately 3500 m and 5000 m have not a physical origin, but stem from the Fourier Transformation, which requires periodicity of the signal.

As can be seen in figure 4, the steeper field gradients in space-domain for the shallow sea situation correspond in the wavenumber-domain to energy at higher wavenumbers compared to the deep sea situation. In other words, if the source is vertically close to the receivers (shallow sea situation), the data has a higher bandwidth than if the source is vertically further away from the receivers (deep sea situation). In figure 4 it can also be seen that the wavenumber spectra of the magnetic and the electric fields behave similarly. The inlets magnify the fields near the zero wavenumber. The fields differ clearly from each other in this area. These differences, combined with the high amplitude and different phase behavior around small wavenumbers, lead to the pronounced differences between the magnetic and the electric fields in the space-domain.

The reflection response $\hat{\mathbf{R}}_0^+$, which is retrieved after decomposition into up- and downgoing fields and MDD, is shown in figure 5 for the shallow sea (dark gray line) and the deep sea situation (light gray line) as a function of offset for different spacings dx . The total offset is kept constant, therefore with increasing spacing dx the number of samples N decreases. Since MDD replaces the water layer with a halfspace, the reflection responses for the shallow sea and the deep sea situation should be identical (in case of correct sampling). The retrieved reflection responses are compared with a directly modeled reflection response (black solid line), which is the exact response when the water layer is replaced by a halfspace.

In figure 5 a) the spacing dx is equal to 2.5 m. Both retrieved reflection responses and the directly modeled reflection response show exactly the same shape verifying that MDD was successful in removing the im-

print of the water layer for both cases. This is also true for a spacing of $dx = 5$ m. A spacing of $dx = 10$ m shows tiny artifacts around zero offset in the shallow sea case, as can be seen in the inlet of figure 5 b). Due to the small amplitude of these artifacts, they can be neglected, but if the spacing is increased further to $dx = 20$ m (figure 5 c), these artifacts at small offsets become more dominant in the shallow sea situation. As seen in figure 3 and mentioned earlier, the electromagnetic fields for the shallow sea case decay faster in the space-domain and have therefore a higher bandwidth in the wavenumber-domain. Increasing the spacing means in the wavenumber-domain to limit the range of wavenumbers. Consequently, a larger spacing introduces aliasing for the high wavenumbers and therefore affects the decomposition algorithm. Improperly decomposed fields lead to artifacts in the retrieved reflection response. A sampling of $dx = 20$ m seems to be too large. For the deep sea situation, the fields decay less strong and therefore this sampling is still sufficient. To detect reservoirs in the subsurface, the small offsets are not of interest, and therefore the artifacts in this region can be ignored. If the spacing is further increased to $dx = 40$ m as shown in figure 5 d), the reflection response for the shallow sea situation is now also for intermediate offsets not retrieved correctly. On the other hand, for the deep sea situation $\hat{\mathbf{R}}_0^+$ could be retrieved perfectly. Further increase of the spacing decreases the quality of $\hat{\mathbf{R}}_0^+$ for the shallow sea situation as expected even more while the reflection response can be retrieved with good quality for the deep sea situation up to a spacing dx equal to 320 m. Artifacts are introduced in the deep sea situation if a spacing of 640 m is reached.

Hunziker *et al.* (2009) show an empirical rule to define the sampling dx as a function of the vertical source-receiver distance z_{sr} . Since the stabilization parameter ε is fixed in their study, but not in this one, their rule can be relaxed. To be precise, the rule presented here is four times less restrictive. Consequently, sampling should be chosen such that $dx \leq z_{sr}/2.5$ to retrieve the reflection response perfectly. If small artifacts around zero offset on $\hat{\mathbf{R}}_0^+$ can be ignored, sampling is sufficient if $dx \leq z_{sr}$. But it should be taken into account, that for bigger sampling distances, the stabilization of the inversion is more difficult. With real data it might not be possible to find the best choice for the stabilization parameter ε and stricter rules should be applied. Fan and Snieder (2009) found a similar rule for electromagnetic fields emitted by a source with a length of 100 m.

5 CONCLUSIONS

SBL data were modeled for a shallow sea and a deep sea situation for a point source. The electromagnetic fields were decomposed and the reflection response $\hat{\mathbf{R}}_0^+$ was retrieved with interferometry by MDD. Different spac-

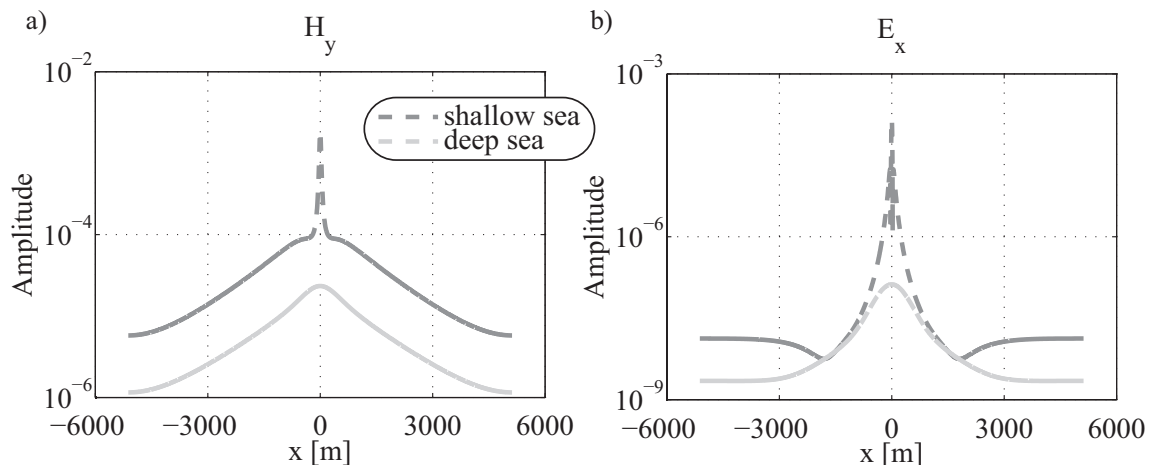


Figure 3. Electromagnetic fields in the space-domain as a function of offset for the shallow sea (dark gray) and the deep sea (lighter gray) situation on a semi logarithmic plot emitted by a point source. a) H_y b) E_x .

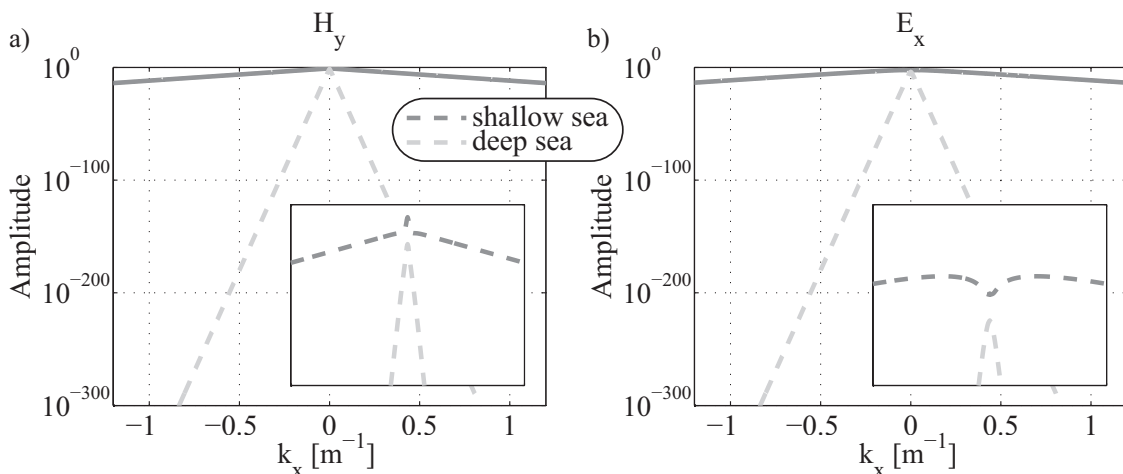


Figure 4. The same electromagnetic fields as in figure 3 in the wavenumber-domain. The insets magnify the fields between -0.1 and 0.1 m^{-1} and amplitudes ranging from 10^{-6} to 10^0 . a) H_y b) E_x .

ings were tested to investigated the required sampling distance.

Although the original electromagnetic fields are strongly affected by the thickness of the water layer, $\hat{\mathbf{R}}_0^+$ is independent of it and consequently identical for the shallow sea and the deep sea situation. In other words, the retrieved reflection response is independent of the source position within the water layer.

In contrast to the reflection response the original electromagnetic fields depend on the vertical source-receiver distance and the source length. The fields decay faster if the vertical source-receiver distance is small (shallow sea situation) compared to a large vertical source-receiver distance (deep sea situation). In the wavenumber-domain this results in a higher bandwidth for the shallow sea data. A higher sampling is required

for the shallow sea case to prevent aliasing and problems in the decomposition of the fields, which finally lead to artifacts in the retrieved reflection response. Consequently the necessary sampling depends on the vertical source-receiver distance.

The necessary sampling distance presented here is, especially for a shallow sea situation, too small for a practical application. To overcome this issue is therefore subject of current research.

ACKNOWLEDGMENTS

This research is supported by the Dutch Technology Foundation STW, applied science division of NWO and

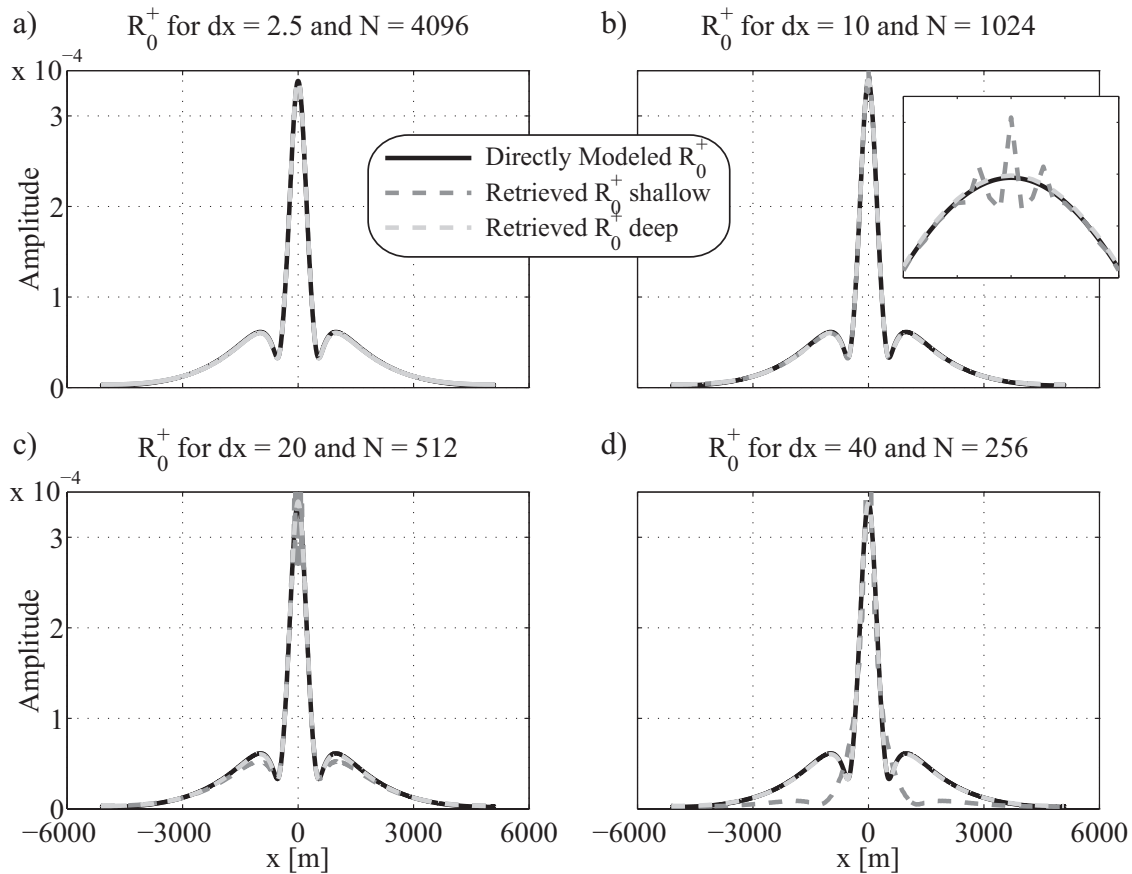


Figure 5. Reflection Responses for different receiver spacings as a function of offset. Spacing dx and the amount of datapoints N is given in the figure captions. The spatial sampling dx is given in meters. The axes span in all plots over the same range. The inlet in subfigure b) magnifies the area between -100 m and 100 m and an amplitude range between 3×10^{-4} and 3.7×10^{-4} .

the Technology Program of the Ministry of Economic Affairs.

REFERENCES

Amundsen, L., Løseth, L., Mittet, R., Ellingsrud, S., & Ursin, B. 2006. Decomposition of electromagnetic fields into upgoing and downgoing components. *Geophysics*, **71**, G211–G223.

Bakulin, A., & Calvert, R. 2006. The virtual source method: Theory and case study. *Geophysics*, **71**, SI139–SI150.

Berkhout, A. J. 1982. *Seismic Migration. Imaging of Acoustic Energy by Wave Field Extrapolation*. Elsevier.

Draganov, D., Wapenaar, K., & Thorbecke, J. 2006. Seismic interferometry: Reconstructing the earth's reflection response. *Geophysics*, **71**, SI61–SI70.

Fan, Y., & Snieder, R. 2009. 3-D Controlled Source Electromagnetic Interferometry by multidimensional deconvolution. *CWP-636, 2009 Annual Project Review Book*.

Hunziker, J., Slob, E., & Wapenaar, K. 2009. Controlled Source Electromagnetic Interferometry by multidimensional deconvolution: spatial sampling aspects in Sea Bed

Logging. *71st EAGE Conference and Exhibition, Expanded Abstracts*.

Schuster, G. 2009. *Seismic Interferometry*. Cambridge University Press.

Schuster, G. T., Yu, J., Sheng, J., & Rickett, J. 2004. Interferometric/daylight seismic imaging. *Geophysical Journal International*, **157**, 838–852.

Slob, E. 2009. Interferometry by Deconvolution of Multicomponent Multioffset GPR Data. *IEEE Transactions on Geoscience and Remote Sensing*, **47**, 828–838.

Slob, E., Draganov, D., & Wapenaar, K. 2007. Interferometric electromagnetic Green's functions representations using propagation invariants. *Geophysical Journal International*, **169**, 60–80.

Snieder, R. 2006. Extracting the Green's function of attenuating heterogeneous acoustic media from uncorrelated waves. *Journal of the Acoustical Society of America*, **121**, 2637–2643.

Wapenaar, K. 2004. Retrieving the elastodynamic Green's function of an arbitrary inhomogeneous medium by cross correlation. *Physical Review Letters*, **93**, 254301–1 – 254301–4.

Wapenaar, K., van der Neut, J., & Ruigrok, E. 2008a. Pas-

- sive seismic interferometry by multidimensional deconvolution. *Geophysics*, **73**, A51–A56.
- Wapenaar, K., Slob, E., & Snieder, R. 2008b. Seismic and electromagnetic controlled-source interferometry in dissipative media. *Geophysical Prospecting*, **56**, 419–434.
- Wapenaar, K., Draganov, D., & Robertsson, J. O. A. (eds). 2008c. *Seismic interferometry: history and present status*. Society of Exploration Geophysicists, Geophysics Reprint Series No. 26.